*Proc. Natl. Acad. Sci. USA*
Vol. 91, pp. 6534–6538, July 1994
Neurobiology

# An array of early differentiating cones precedes the emergence of the photoreceptor mosaic in the fetal monkey retina

KENNETH C. WIKLER AND PASKO RAKIC

Section of Neurobiology, Yale University School of Medicine, 333 Cedar Street, New Haven, CT 06510

*Contributed by Pasko Rakic, February 28, 1994*

ABSTRACT **We previously have demonstrated that ≈10% of cones in the fetal monkey retina precociously express the red/green opsin. These data suggested the possibility that a subset of cones differentiates prior to their nascent cone neighbors. To further assess this early cone differentiation in the fetal monkey retina, we used monoclonal antibodies proven to be important developmental markers of photoreceptor phenotypes and synaptogenesis (XAP-1, specific to photoreceptor membranes; SV2, specific to synaptic vesicle protein). Although these two antibodies recognize functionally distinct antigens, our analyses revealed that both identify a subset of precociously immunoreactive cones. Further, XAP-1- and SV2-positive cones are distributed in the same pattern as precocious red/green-sensitive cones in immature regions of the fetal monkey retina. These results support the hypothesis that the primate retina possesses a spatially organized protomap that may induce the emergence of the photoreceptor mosaic and trigger the formation of color-specific pathways that include horizontal, bipolar, and retinal ganglion cells.**

The vertebrate retina is composed of seven major neuronal classes, several of which are further subdivided into functionally, chemically, and morphologically distinct cell subtypes. Photoreceptors, for example, consist of rods and cones. In the retina of diurnal primates, including humans, cones are further subdivided into three subtypes, the red-, green-, and blue-sensitive cones, whose visual pigments are maximally sensitive to long, middle, and short wavelengths, respectively (1). The development of opsin-specific antisera has permitted the quantitative assessment of the distribution of these wavelength-sensitive cones in several different primates, revealing stereotypical and species-specific distributions of cone subtypes across the retinal surface (2–4). In the rhesus monkey, for example, the opsin-specific cone subtypes are arranged in a reiterative pattern or mosaic in which single blue-sensitive cones are surrounded by ≈10 red/green-sensitive cones (3). However, the cellular mechanisms that control the differentiation and deployment of wavelength-sensitive cones within these complex patterns are not known.

Previous studies in our laboratory have used opsin-specific antibodies to chart the development of the mosaic of the red/green- and blue-sensitive cone subtypes in the fetal monkey retina. Using an antibody specific to the red/green opsin (5), our initial studies revealed that a small number of red/green-sensitive cones (about 10% of the adult number) are immunopositive at least 3 weeks prior to the emergence of immunoreactivity in the surrounding, postmitotic cones (6). The goal of the present study was to determine whether these subsets of cones display a similar pattern of accelerated maturation for other biochemical and morphological characteristics. The monoclonal antibodies used to address this question included XAP-1, which recognizes photoreceptors in the *Xenopus* retina and has been used in monitoring the differentiation of photoreceptor phenotypes (7), and SV2, which recognizes synaptic vesicle protein and has served as a sensitive marker for the development of functional synapses in the fetal monkey retina (8). The present results indicate that these two immunolabels recognize antigens localized to distinct subcellular compartments in immature cones, and each is expressed precociously in ≈10% of all cones. These cone subsets may well correspond to the same population that precociously expresses the red/green opsin. Thus, the array of early differentiating red/green-sensitive cones may be visualized by multiple criteria, suggesting that this group of early maturing cells may be important for the emergence of the mosaic of red-, green-, and blue-sensitive cones in the primate retina.

## MATERIALS AND METHODS

**Tissue Preparation.** Retinae from five fetuses obtained at midgestation and two adult rhesus monkeys (*Macaca mulatta*) were used. Fetuses were removed by cesarean section, deeply anesthetized with ketamine and sodium pentobarbital, and killed at embryonic (E) days E65, E80, E90, E110, or E120. Dissected retinae were marked for orientation and fixed in 4% paraformaldehyde in 0.1 M phosphate buffer (pH 7.4). One retina from each animal was prepared as a whole mount and processed for immunocytochemistry. The other retina was cut serially at 10-μm thickness on a cryostat and mounted onto coated slides.

**Immunohistochemistry.** Fixed retinal whole mounts and cryostat sections were first rinsed in 0.1 M phosphate buffer and then incubated overnight with either XAP-1, an IgM monoclonal antibody diluted 1:500 with 0.1% Triton X-100 in 0.1 M phosphate buffer (pH 7.4), or SV2, a monoclonal antibody diluted 1:10,000 with 0.1% Triton X-100 in 0.1 M phosphate buffer (pH 7.4). After a 16-h incubation at 4°C, tissue was incubated in either biotinylated anti-mouse IgG or IgM (1:200) for 1 hr at 22°C. The retinae were then rinsed in phosphate buffer and incubated in an avidin–biotin–peroxidase complex (Vectastain, Vector Laboratories) for 1 hr prior to being visualized in 0.05%, 3,3-diaminobenzidine hydrochloride/0.003% $H_2O_2$. Retinae were mounted photoreceptor side up onto coated slides, placed in a glycerin solution, and protected with coverslips.

**Sampling.** From the serial cryostat sections, at least six equally spaced retinal samples were treated with each of the antibodies for assessment of immunoreactivity: two sections were taken superior to the optic disc, two sections through the optic disc, and two sections ventral to the optic disc. To compare laminar and areal distributions of immunoreactive cones, reconstructions of cryostat sections were compared with companion retinal whole mounts taken from the other eye. Cell counts of antibody-treated retinal whole mounts were made every 0.5 mm with a ×100 oil-immersion objective with a final magnification of ×2600 (see ref. 3).

The publication costs of this article were defrayed in part by page charge payment. This article must therefore be hereby marked "*advertisement*" in accordance with 18 U.S.C. §1734 solely to indicate this fact.

Abbreviation: OPL, outer plexiform layer.

## RESULTS

**Adult Distribution of XAP-1 and SV2 Immunoreactivity.** Both the XAP-1 and SV2 antigens are present in the adult monkey retina and have unique topographic and intracellular distributions. Examination of retinal whole mounts revealed that XAP-1 immunoreactivity is restricted to cones. Quantitative analysis of the distribution of XAP-1-positive cones showed that 90% of all cones are labeled in the adult retina. In tangential sections, XAP-1 immunoreactivity was localized within the inner and outer segments of cones and cone pedicles in the outer plexiform layer (OPL).

Immunoreactivity for the SV2 antibody was concentrated exclusively in two synaptic layers: the outer and inner plexiform layers. SV2 immunoreactivity was uniformly dense throughout the OPL and labeled the synaptic endings of both rods and cones (see also ref. 8). Examination of whole mounts and transverse sections confirmed that both the inner and outer segments of all rods and cones were immunonegative for SV2 in the adult rhesus monkey retina.

**Development and Cellular Localization of XAP-1 Immunoreactivity.** The first XAP-1-immunopositive profiles were restricted to the OPL in foveal and perifoveal regions of the E70 retina (Fig. 1*A*). The periodic spacing of immunoreactivity in the OPL suggested that XAP-1-positive profiles corresponded to the synaptic pedicles of immature cones. At E90, strong immunolabeling in the OPL (Fig. 1*B*) contrasted with weakly XAP-1-immunoreactive cone inner segments, which were identified occasionally in central retinal regions. In the E110 and E120 retinae, XAP-1 immunoreactivity became markedly attenuated in the OPL, while dramatically increasing over the cone inner segments (Fig. 1*C*). Thus, the density of XAP-1 immunoreactivity, which was initially concentrated in the OPL and weak over cone inner segments, essentially reversed by E120 when immunolabeling was weak over the OPL and was most prominent over the cone inner segments.

**Development and Cellular Localization of SV2 Immunoreactivity.** The most striking feature of SV2 labeling in the fetal monkey retina was the transient appearance of immunoreactivity in the nonsynaptic layers of the retina, specifically in the outer nuclear layer. SV2 labeling in the fetal photoreceptor layer appeared to shift in expression from the apical segment of immature cones at E70 to their synaptic pedicles in the OPL by E110 (Fig. 1 *D–F*). The first SV2-positive cone pedicles were found in the foveal and perifoveal regions of the E70 retina, while in the less mature periphery of the same retina, SV2 immunoreactivity was found only within the apical segments of immature cones (Fig. 1*D*). By E90, SV2-immunoreactive cone pedicles were found across the entire retina, and a dense and continuous band of SV2-immunoreactivity was present over the cone inner segments in this specimen (Fig. 1*E*). However, immunoreactivity to the SV2 antibody virtually disappeared from the inner segments and cell bodies of cones in central retinal regions by E110. By E120, SV2 immunoreactivity was localized exclusively in the OPL across the entire retina (Fig. 1*F*).

**Topographic Distribution of XAP-1 and SV2 Across the Fetal Retina.** Examination of fetal retinal whole mounts revealed a pronounced center-to-peripheral progression in the emergence and shifting of immunoreactivity to both XAP-1 and SV2 antibodies. For example, the proportion of cones that were XAP-1 immunopositive varied systematically according to retinal eccentricity. In a 20-mm$^2$ area centered on the fovea of the E90 retina, ≈90% of all cones were strongly XAP-1 immunopositive—a ratio of labeled to unlabeled cones similar to that seen in the adult (Fig. 2*A*). Immediately surrounding the foveal region, a similar proportion of cones were XAP-1 immunopositive. However, a few labeled cones always stood out in this less mature region as more strongly immunoreactive than their neighbors (Fig. 2*B*). In peripheral regions of the same whole mount, only 10% of the cones were immunoreactive, and these cells were regularly distributed so

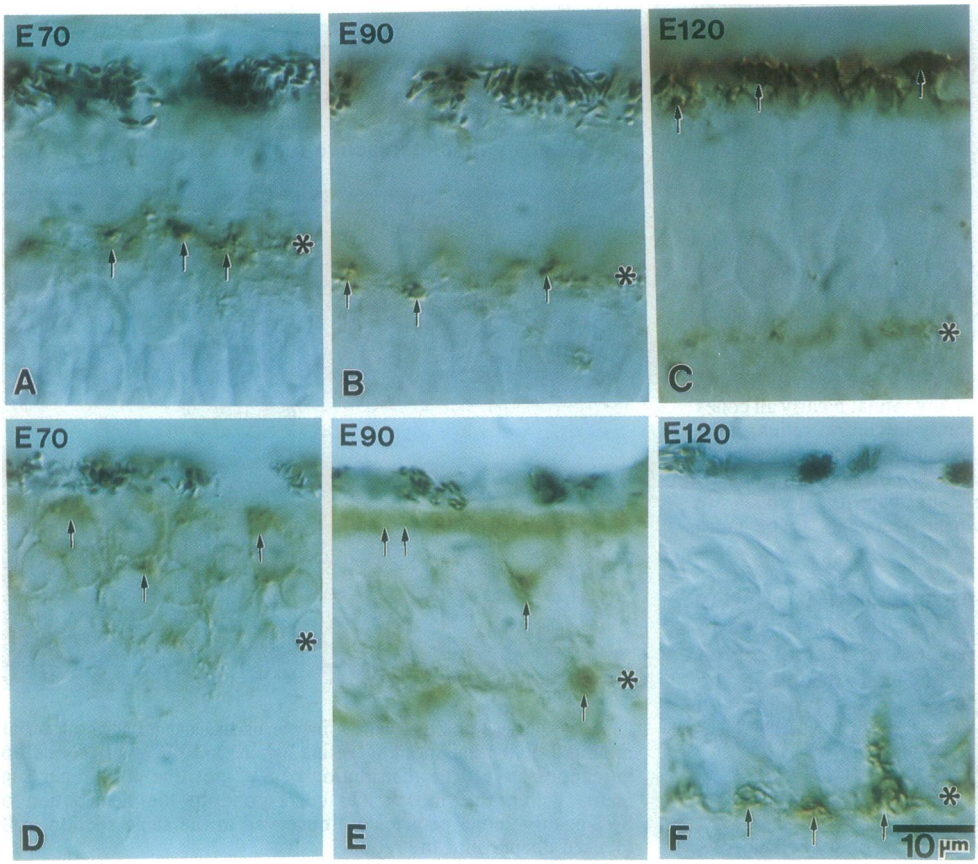


FIG. 1. Coronal sections from fetal monkey retinae at E70 (*A* and *D*), E90 (*B* and *E*), and E120 (*C* and *F*) processed for immunocytochemical visualization of XAP-1 (*A–C*) and SV2 (*D–F*). XAP-1-positive profiles (arrows) are confined to the OPL at early fetal ages but are found predominantly at the level of the cone inner segments by E120. SV2 immunoreactivity (arrows) is found predominantly at the apical segments of immature cones at E70 but is restricted to cone pedicles by E120. Asterisk indicates the OPL.

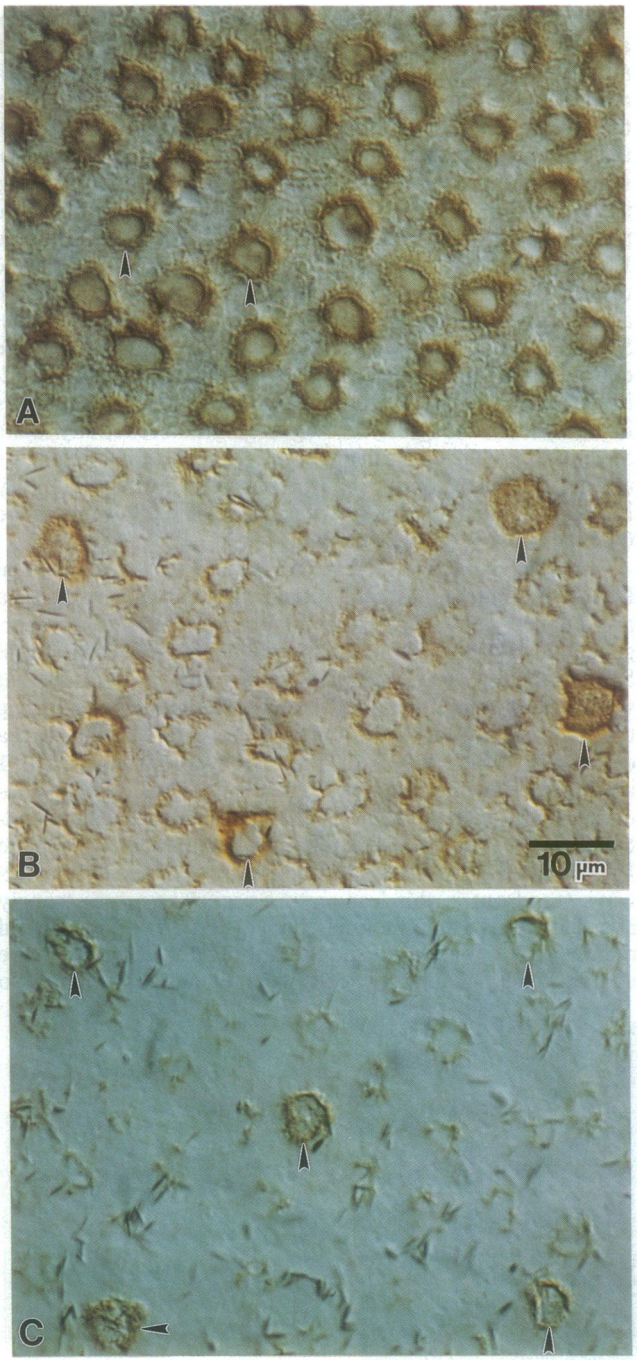


FIG. 2. XAP-1-positive cones in central (*A*), pericentral (*B*), and peripheral (*C*) regions of an E90 fetal monkey retina. Nearly all cones are immunoreactive to the XAP-1 antibody in central retina; however, only 10% of all cones are XAP-1 positive (arrowheads) in the periphery of the same retina. The area between these two regions (*B*) appears to be a transition zone, where the majority of cones are immunoreactive, but a subset (arrowheads) appears to be more heavily labeled than their neighbors.

that each immunopositive cone was surrounded by roughly 10 to 15 unlabeled cones (Fig. 2*C*). This ratio of labeled to unlabeled cones was nearly the inverse of that observed perifoveally. No XAP-1-positive cones were found in the most immature margins of the E90 retina. In E110 and 120 retinae, ≈90% of cones across most of the retina were densely immunoreactive for XAP-1. Only in regions restricted to the peripheral rim of these retinae were solitary XAP-1-positive cones surrounded by ≈15 unlabeled cones. The mature pattern of XAP-1-labeling was observed across the entire retina, including the peripheral-most margins only after E120. These disparate patterns in mature vs. immature retinal subdivisions suggest that XAP-1 immunoreactivity emerges first within a subpopulation of cones.

SV2 immunocytochemistry also revealed a restricted distribution of prematurely immunoreactive cones, which could be identified in retinal whole mounts at E90 and E110. For example, in E90 retinae peripheral to the perifoveal area, an array of single SV2-positive cone inner segments was found, each surrounded by ≈12 neighboring unlabeled cones (Fig. 3*A*). In concentric foveal and parafoveal regions, cone inner segments were no longer immunopositive because SV2-labeling had become restricted to synapses in the OPL. Sandwiched between these two regions was an apparent transition zone in which the majority of cone inner segments were immunoreactive to the SV2 antibody. In immature regions of the periphery of the E90 retina, it was more difficult to identify SV2-positive cones because only the apical tips of these cells were immunoreactive. By E120, SV2 immunoreactivity was completely restricted to the OPL layer.

The identification of a regularly distributed subset of precociously SV2-positive cones indicates that these cells may form synapses prior to their neighbors. To determine whether these cones possess immunoreactive synaptic pedicles, we used an oil-immersion objective (×100, 1.32 n.a.) to examine the entire length of individual labeled and unlabeled cones within these whole-mount preparations. This analysis revealed an identical number and arrangement of SV2-positive cone pedicles (Fig. 3*B*) 20–25 μm vitreal to the array of SV2-positive cone inner segments (Fig. 3*C*). Previous electron microscopic examination of the fetal monkey retina (8, 9) suggests that the developmental onset of SV2 immunoreactivity correlates with the appearance of morphologically mature synapses. Taken together these data suggest that the subset of cones precociously immunoreactive to the SV2 antibody may indeed form synapses in the OPL prior to neighboring cones.

## DISCUSSION

**Early Differentiating Cones in the Fetal Monkey Retina.** The results of this study show that ≈10% of all cones are precociously immunoreactive for the XAP-1 antibody (spe-

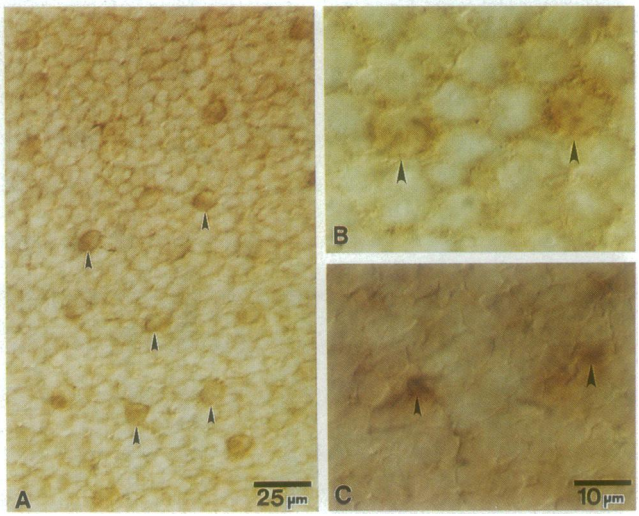


FIG. 3. SV2-positive cones in peripheral (*A*) regions of a flat-mounted E90 fetal monkey retina where ≈10% of all cones are immunoreactive. The distribution of SV2-positive cone inner segments within this mosaic (*B*) correspond to the distribution of SV2-positive cone pedicles (*C*) observed in the same section, roll-focused deeper into the retina.

cific to cone membranes) and the SV2 antibody (specific to synaptic vesicle protein). These similarities in the ratios and arrangements of precociously immunoreactive cones are significant given the distinctly different phenotypic features recognized by these markers. In addition, these markers demonstrated opposing developmental shifts in radial distribution: immunoreactivity to the SV2 antibody shifted inwardly from the apical segment of immature cones to their pedicles in the OPL, whereas immunoreactivity to the XAP-1 antibody appeared to shift outwardly from the OPL to the cone outer segments. Thus, although these functionally distinct phenotypic features are expressed concurrently during retinal development, the dynamics of their intracellular compartmentalization may be differentially regulated.

The present data are concordant with our previous observation that 10% of all cones precociously express the red/green opsin (6) and suggest that XAP-1 and SV2 may identify the same set of early differentiating red/green-sensitive cones. However, a recent analysis of blue-sensitive cones in the fetal monkey retina using an opsin-specific monoclonal antibody (OS-2) (10) revealed the presence of blue-sensitive cones in the fovea at E83, 3 weeks earlier than we previously reported using a blue-opsin-specific polyclonal antisera (108B) (6). This result raised the possibility that blue-sensitive cones might also emerge earlier than previously shown in less mature, peripheral regions of the fetal retina. We have reexamined the distribution of blue-sensitive cones in E80 and E90 monkey retinal whole mounts using the OS-2 antibody. Importantly, these analyses have failed to produce evidence for a population of early differentiating blue-sensitive cones. We conclude that the population of early differentiating cones identified by the SV2 and XAP-1 antibodies correspond to those cells that precociously express the red/green opsin.

Does the precocious formation of synapses in the OPL influence the expression of the red/green opsin by a subset of cones? A number of observations suggest that the expression of a wavelength-sensitive photopigment may be independent of synaptic interactions between cones and either horizontal or bipolar cells. First, while precocious red/green-sensitive cones are found in the periphery of the E80 fetal monkey retina (6), synaptogenesis in this region does not occur until approximately E110 (8, 9). In addition, several *in vitro* studies have demonstrated that individual rods cultured in isolation (thus prevented from making direct contact with other retinal cell types) can nevertheless differentiate and express rhodopsin (11). These reports strongly suggest that the determination of opsin-specific phenotypes occurs independently and prior to synaptogenesis.

One interpretation of our results is that the array of early differentiating cones in the rhesus monkey may direct the specification of the opsin phenotype of surrounding nascent cones, perhaps through nonsynaptic cellular interactions, and thus may act as a scaffold for the development of the adult mosaic of red-, green-, and blue-sensitive cones. Three transient features of the immature retinal mosaic support a role for cone–cone interactions in the specification of cone subtypes. First, opsin expression in the fetal monkey retina is detected months after the final mitosis of cones (6, 8). Although immunocytochemical data have indicated that the time of commitment of an immature cell to become either a rod (12) or retinal ganglion cell (13) occurs soon after its final mitotic division, an embryonic cell in the fetal monkey retina may wait up to 2 months after its final mitotic division before expressing a functionally distinct opsin phenotype. Second, in immature regions of fetal primate retinae, cones are not separated from one another by rod inner and outer segments as they are in the adult but are directly apposed to one another (6, 14). Electron microscopic analyses confirm this observation and, in addition, reveal that transient specialized contacts are formed between the membranes of adjacent cones (15). Thus, the organization of the early photoreceptor mosaic may allow transient cone–cone interactions prior to the expression of cone-specific photopigments. Finally, the identification of an array of early differentiating red/green-sensitive cones suggests that this cone subtype, in particular, may be important in mediating cone–cone interactions in the emergence of the mosaic of cone subtypes in the primate retina.

**Model for the Development of Photoreceptor Mosaics.** The most comprehensive examination of pattern formation of a cell mosaic has been described in studies of the development of ommatidia in the compound eye of *Drosophila melanogaster* (reviewed in refs. 16 and 17). The relative position of immature photoreceptors in each ommatidium controls the specification of cell fate in this invertebrate mosaic. For example, the position of an immature pluripotent cell relative to the differentiated R8 photoreceptor determines which of the equivalent cells will differentiate into the R7 photoreceptor. Through signaling mechanisms that act only over short distances, the early position of an undetermined postmitotic cell in an ommatidium seems to control its eventual cell fate.

Several features of the specification of photoreceptor phenotypes in the mammalian retina appear analogous to the development of photoreceptors in *Drosophila melanogaster*. This raises the possibility that the position of an immature photoreceptor may serve as an evolutionarily conserved mechanism that influences the emergence and organization of the reiterative mosaic of cone subtypes. Specification of photoreceptor phenotypes in both systems appears to involve inductive signals that act over short distances (11, 18). The limited range of effectiveness of these signals makes the position of an uncommitted cell of paramount importance in determining its eventual fate in the invertebrate mosaic and potentially within the mammalian retina as well. A second similarity in the development of these systems is the early differentiation of an array of photoreceptors that may utilize these putative signals and thus organize the differentiation of other photoreceptor subtypes (present study; ref. 6).

Our working model posits that the species-specific organization of the primate mosaic of cone subtypes emerges according to a progressive central-to-peripheral wave of locally restricted interactions among adjacent cones (Fig. 4). This series of inductive events takes place during a fetal period when postmitotic cones are in the majority but have not expressed their opsin-specific photopigments. During this period the immature photoreceptor mosaic resembles a honeycomb arrangement of postmitotic cones that seems to consist of repeating cellular assemblies of early differentiating red/green-sensitive cones surrounded by 10–15 pluripotent cones (Fig. 4). This model assumes that the position of each undetermined cone relative to the closest precocious profile determines if it will differentiate into either the red/green- or blue-opsin-specific phenotype. Specifically, an early differentiating, red/green-sensitive cone, through a distance-limited signal, will trigger pluripotent cones situated within its local domain to differentiate into the red/green-opsin phenotype. Those pluripotent cones located farther from an early differentiating cone will be exposed to less of this putative signal and, consequently, will follow a default pathway and differentiate into the blue-opsin phenotype. Thus, a distance-dependent mechanism enables the array of early differentiating red/green-sensitive cones to serve as a template for the development of the mosaic of cone subtypes.

The mature phenotype of red-, green-, or blue-sensitive cones is characterized not only by differences in the expression of a wavelength-sensitive opsin but also in the formation of subtype-specific synaptic contacts. Red/green and blue-sensitive cones form synaptic contacts specifically with different subtypes of bipolar cells in the mammalian retina (19).

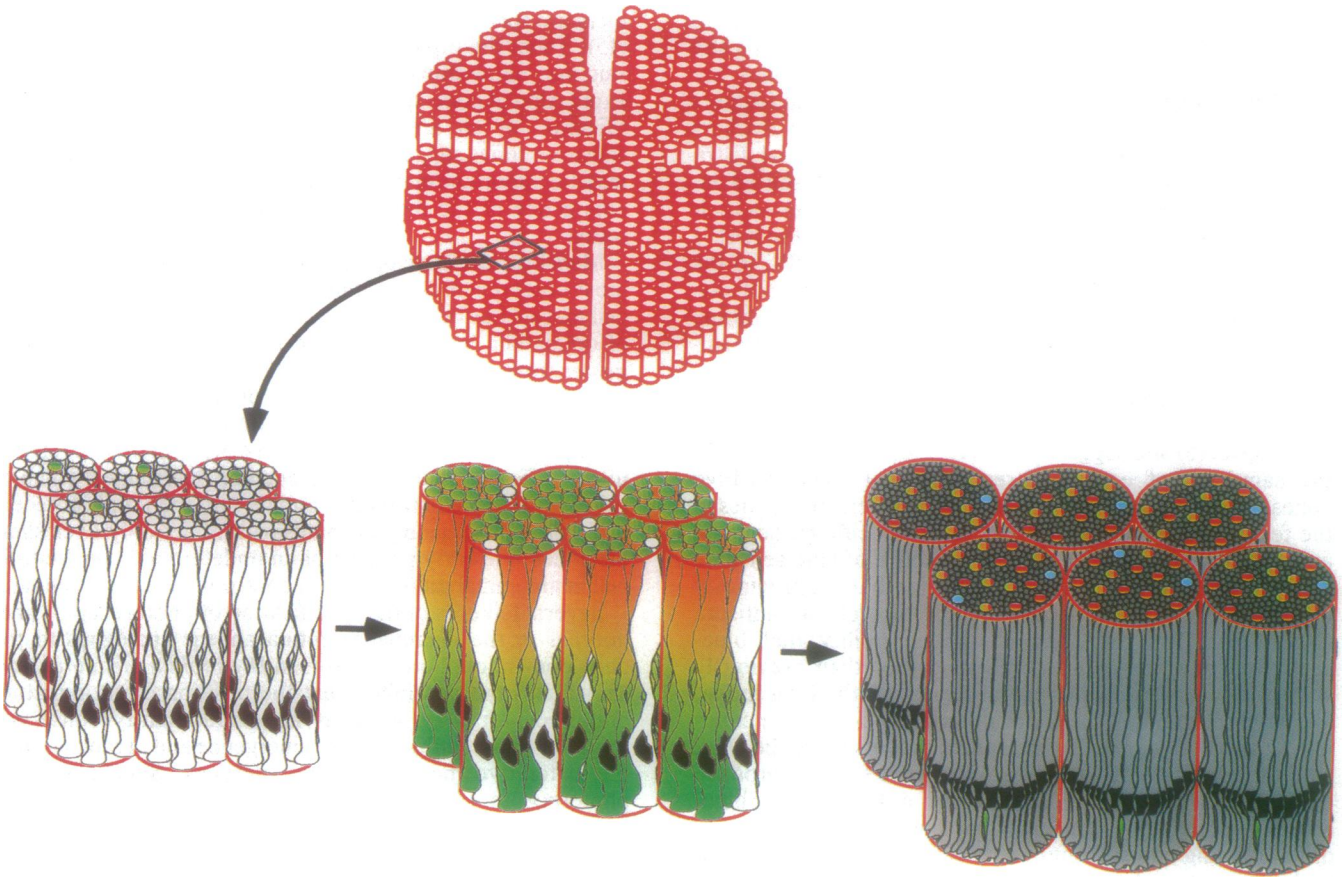

FIG. 4. A schematic diagram illustrating a working model of the emergence of the opsin-specific cone subtypes and the dynamic transition from an all-cone mosaic to a rod–cone mosaic based on ref. 6 and the present data (see text for details).

In addition, cone subtypes can be distinguished by differences in the composition of their cellular membranes. For example, the monoclonal antibody CSA-1, which recognizes a carbohydrate moiety in cone membranes (20), specifically identifies red/green-sensitive, but not blue-sensitive cones (3). The present results indicate that the maturation of these three phenotypic characteristics emerges in a similar geometric pattern. It is conceivable that this distance-dependent mechanism could apply equally to the determination of a cone's class-specific opsin, synaptology, and membrane properties.

We hypothesize that the transient array of early differentiating cones reflects the earliest spatial organization of cells in the fetal monkey retina and participates in the emergence of cellular arrays in all layers of the primate retina. It should be emphasized, however, that the emergence of this primordial map occurs prior to the formation of synaptic connections between the retina and central structures in the visual system. Moreover, different centers within the visual system contain independent protomaps that foreshadow the species-specific organization of neuronal circuits. For example, the stereotypical size and spacing of chromatically selective cells positioned within cytochrome oxidase blobs in the visual cortex can emerge in the absence of cues from retinal photoreceptors (21). These studies suggest that both cortex (22) and retina (6) contain protomaps of their species-specific organization, but how these maps interact via geniculate relay in the thalamus remains to be determined.

We thank Drs. W. Harris (University of California), K. Buckley (Harvard University), and A. Szel (Semmelweis University of Medicine, Budapest) for their gifts of the XAP-1, SV2, and OS-2 antibodies. The work was supported by Grants EY09917 (to K.C.W.) and EY02593 (to P.R.) from the National Institutes of Health.

1. Jacobs, G. H. (1981) *Comparative Color Vision* (Academic, New York).
2. Szel, A., Diamantstein, T. & Rohlich, P. (1988) *J. Comp. Neurol.* **273**, 593–602.
3. Wikler, K. C. & Rakic, P. (1990) *J. Neurosci.* **10**, 3390–3401.
4. Curcio, C. A., Allen, K. A., Sloan, K. R., Lerea, C. L., Hurley, J. B., Klock, I. B. & Milam, A. H. (1991) *J. Comp. Neurol.* **312**, 610–624.
5. Lerea, C. L., Bunt-Milam, A. K. & Hurley, J. B. (1989) *Neuron* **3**, 367–376.
6. Wikler, K. C. & Rakic, P. (1991) *Nature (London)* **351**, 397–400.
7. Harris, W. & Messersmith, S. (1992) *Neuron* **9**, 357–372.
8. Okada, M., Erickson, A. & Hendrickson, A. (1994) *J. Comp. Neurol.* **339**, 535–558.
9. Nishimura, Y. & Rakic, P. (1987) *J. Comp. Neurol.* **262**, 290–313.
10. Bumsted, K., Hendrickson, A., Erickson, A. & Szel, A. (1993) *Neurosci. Abstr.* **19**, 52.
11. Altshuler, D. & Cepko, C. (1992) *Development* **114**, 947–957.
12. Barnstable, C. J. (1987) *Immunol. Rev.* **100**, 47–78.
13. McLoon, S. C. & Barnes, R. B. (1989) *J. Neurosci.* **9**, 1424–1432.
14. LaVail, M. M., Rapaport, D. H. & Rakic, P. (1991) *J. Comp. Neurol.* **309**, 86–114.
15. Wikler, K. C. & Rakic, P. (1992) *Neurosci. Abstr.* **18**, 1317.
16. Ready, D. F. (1989) *Trends Neurosci.* **12**, 102–110.
17. Greenwald, I. & Rubin, G. M. (1992) *Cell* **68**, 271–281.
18. Watanabe, T. & Raff, M. C. (1992) *Development* **114**, 899–906.
19. Marshak, D. W., Aldrich, L. B., Del Valle, J. & Yamada, T. (1990) *J. Neurosci.* **10**, 3045–3055.
20. Johnson, L. V. & Hageman, G. S. (1988) *Invest. Ophthalmol. Visual Sci.* **29**, 550–557.
21. Kuljis, R. O. & Rakic, P. (1990) *Proc. Natl. Acad. Sci. USA* **87**, 5303–5306.
22. Rakic, P. (1988) *Science* **241**, 170–176.